Available online at www.eccomasproceedia.org
Eccomas Proceedia COMPDYN (2023) 2476-2491

ECCOMAS Proceedia

COMPDYN 2023
9th ECCOMAS Thematic Conference on
Computational Methods in Structural Dynamics and Earthquake Engineering
M. Papadrakakis, M. Fragiadakis (eds.)
Athens, Greece, 12-14 June 2023

# 3D EXPLORATION OF INTERNAL STRESSES DUE TO LATERAL LOADS AND FOUNDATION MOVEMENTS IN A SEMICIRCULAR ARCH

**Antonino Iannuzzo[1*], Antonio Gesualdo[2], Carlo Olivieri[3], Andrea Montanino[2]**

[1] DING - University of Sannio

Piazza Roma 21, 82100 Benevento, Italy

aniannuzzo@unisannio.it

[2] Department of Structures for Engineering and Architecture, University of Naples Federico II

Via Claudio 21, 80125 Napoli, Italy

{gesualdo, andrea.montanino}@unina.it

[3] University of Salerno, Department of Civil Engineering

Via Giovanni Paolo II, 132, 84084 Fisciano (SA), Italy

colivieri@unisa.it

**Abstract**

*The paper explores the internal stress states of masonry structures as composed of no-tension material using an energy-based variational criterion. The numerical formulation directly considers general boundary conditions in terms of loads and displacements and treats the structure as an assembly of rigid bodies, resulting in a three-dimensional partition of the structural domain. The analysis is performed on the interfaces defined by this partition to determine internal forces in equilibrium with given external loads and compatible with potential non-zero boundary displacements.*
*The mechanical problem is formulated as the Total Complementary Energy (TCE) minimum, which is then discretized and framed into a Linear Program (LP) or a Second-Order Cone Program (SOCP). The TCE objective function considers the non-homogeneous boundary conditions, while the problem's constraints enforce equilibrium and material compatibility conditions represented by a Mohr-Coulomb criterion. The solution to this minimum problem provides*

ISSN:2623-3347 
Peer-review under responsibility of the organizing committee of COMPDYN 2023.
doi: 10.7712/120123.10576.21345

*internal, admissible, equilibrated stress states that are also compatible with non-zero boundary displacements. It is shown how different boundary conditions can drastically influence and re-direct the internal stress states, and, thus, the internal force pattern. Importantly, the use of foundation settlements allows to explore set of statically admissible stress and thus to define the resilience of the structure to the variation of external actions.*

**Keywords:** Masonry structures · Unilateral contact problems · Settlements · Internal stress states · Limit Analysis · Flow of forces · Force pattern.

# 1 INTRODUCTION

URM structures make up a significant proportion of residential buildings and many historical monuments that possess high architectural value. Because of their vulnerability, significant research effort has been dedicated to developing techniques that can preserve URM structures for future generations as a testament to our cultural heritage over the last few decades. However, addressing the mechanical issues associated with these structures is a complicated and highly non-linear task. URM structures exhibit unilateral behaviour, often experience fractures due to settlements, and the boundary conditions are frequently unknown or unknowable. Consequently, evaluating these structures represents a highly complex task.

Currently, it is widely acknowledged that the unilateral behaviour of masonry cannot be overlooked, and the use of a non-negligible tensile capacity may lead to erroneous conclusions [1, 2]. This realization poses new challenges, particularly in numerical methods, as the standard and efficient techniques suitable for bilateral materials cannot be applied. Therefore, numerous numerical approaches have been developed and employed over the years to study and evaluate old masonry structures. Specifically, Finite Element (FE) methods with specialized and sometimes intricate constitutive material relations have been proposed for their capability to handle complex mechanical and geometric issues [3, 4, 5]. Discrete Element Modelling (DEM) methods [6] have also been widely utilized due to their capacity to tackle challenging 3D problems. DEM methods necessitate a model composed of a finite number of blocks that can move independently, enable large displacements, allow contact opening, and the formation of new contacts between blocks (even those that were previously not in contact). DEM techniques employ an explicit dynamics time-stepping procedure that makes the problem computationally intensive. For further details, the reader may refer to [7, 8, 9, 10, 11, 12]. The primary disadvantage of both FE and DEM methods is that they are often computationally demanding and necessitate a detailed description of the mechanical properties of the material that may, at times, be part of the problem in old masonry structures.

To address the challenges in assessing masonry structures, Limit Analysis methods have gained widespread acceptance. These methods rely on upper and lower bound formulations, significantly reducing the number of mechanical parameters required (in some cases, only the friction angle or the compressive strength is needed [13]. Non-associative, Limit analysis-based approaches [14, 15, 16, 17], are primarily inspired by Livesley's seminal works [18, 19] and view the masonry as a collection of rigid blocks in unilateral frictional contact. They employ force-based approaches and define displacements as the dual of the primal lower bound problem. The solution is guaranteed when dilatancy phenomena are absent, and the desired convergence is achieved. Narrowing down the attention to standard lower-bound Limit-Analysis approaches, modern research starts thanks to the seminal work of Jacques Heyman [20], who posed the basis for the rigorous modern application of Limit Analysis [21, 22]. Heyman assumptions allow characterising a material without using any mechanical parameter. Lower bound formulations are based on "his" Safe Theorem: if an admissible stress state lying within the material geometry can be found, the structure is in a safe configuration [23]. In recent years, many approaches have been developed to apply the Safe Theorem to complex 3D structures, such as those based on a pure compressive network of forces [24, 25, 26, 27, 28, 29], membrane or thrust surface analysis [30, 31, 32, 33, 34, 35, 36, 37], or in plane behaviour of panels and facades [38, 39, 40, 41].

In the current scientific field, accurately modelling the effects of settlements is still an open topic and a critical issue for assessing masonry structures. Recent contributions to scientific literature have focused on this topic, as small foundation displacements can significantly alter internal stress states, leading to strong non-linear effects. The reader is referred to [42, 43, 44, 45, 46, 47, 48]. Standard Limit Analysis methods based on lower bound formulations are incapable of defining internal stress states as a function of foundation displacements, which is crucial when assessing the thrust exerted on boundary or secondary structures or understanding the working condition of the structure when foundation displacement can be measured.

This paper proposes direct energy-, force-based strategy that provides as solutions internal equilibrated stress states that are also compatible with prescribed foundation displacements. The method is applied to 3D masonry structures and is based on the minimum of the Total Complementary Energy (TCE). The first use and proof of the total complementary energy in solving the equilibrium problem with non-zero displacement data involving normal, rigid material can be traced back to [49]. Moreover, for 2D masonry structures, it was already applied as linear programming (LP) problem and in in [50] for small displacements, and in [51] for large displacement fields. However, in both cases, it was obtained and used as the dual LP problem of the discretised version of the minimum of the total potential energy through the PRD approach [52, 53]. Here, a direct use of this minimum criterion extended to 3D structures is proposed. A partition of the structural domain defined by a suitable set of polyhedral elements is the starting point. The contact among the elements of the partition is supposed to happen only on interfaces' vertices as in a classical concave formulation [19]. The problem is discretized and can be solved in 2D as a Linear Program (LP) or in 3D as a Second-Order Cone Program (SOCP). The difference between these two numerical discretisations is due to the discretization of the Mohr-Coulomb cone, which is linear for plane problems or a 3D cone for a fully 3D model of a structure. Once the numerical method is introduced, various mechanical problems are addressed to demonstrate how different boundary conditions can significantly alter the internal stress states and force patterns. A simple masonry arch is used to clearly demonstrate the proposed method.

## 2 MATERIALS AND METHODS

This Section illustrates the essential mathematical ingredients at the base of the proposed numerical strategy. A 3D continuum masonry structure $\Omega \subset \mathbb{R}^3$ is partitioned into M elements as:

$$(\Omega_i)_{i \in \{1, \ldots, M\}} \,. \tag{1}$$

The contact among the elements is unilateral and follows a Mohr-Coulomb friction-associated flow rule. The two open, disjoint parts $\partial\Omega_U$, $\partial\Omega_F$ represent the constrained and loaded part of the boundary of $\Omega$; while $\partial\Omega_I$ is the union of $\partial\Omega_{I_i}$ for $i \in \{1, \ldots, M\}$, i.e. the union of the interfaces shared by two adjacent elements of (1). Prescribed displacements are applied on $\partial\Omega_U$:

$$\mathbf{u} = \bar{\mathbf{u}} \,, \tag{2}$$

while on $\partial\Omega_F$:

$$\mathbf{s}(\mathbf{T}) = \bar{\mathbf{s}} \,, \tag{3}$$

with $\mathbf{s}(\mathbf{T})$ the trace of $\mathbf{T}$ on the boundary. **Fig. 1** gives an overview of the problem and its mathematical representation referring to a continuum decomposed into two elements.

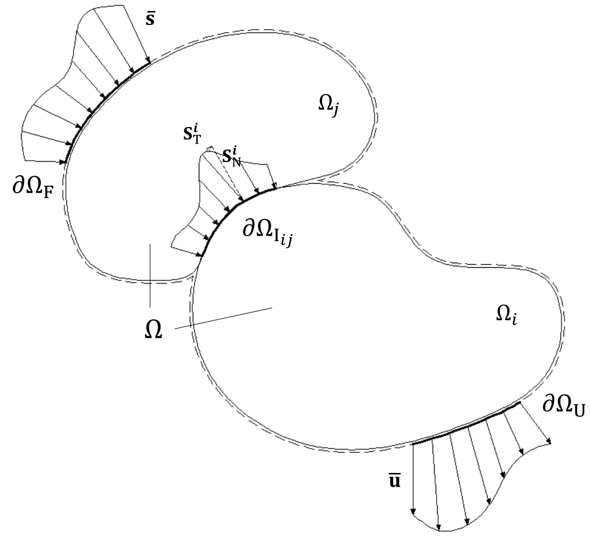


**Fig. 1** – An elastic body $\Omega$ subjected to body forces b, prescribed boundary displacements $\bar{\mathbf{u}}$ on $\partial\Omega_\mathrm{U}$, friction boundary condition on $\partial\Omega_\mathrm{I}$ with given normal $\mathbf{S}_\mathrm{N}$ and tangential $\mathbf{S}_\mathrm{T}$ pressures, and to surface forces $\bar{\mathbf{s}}$ on the $\partial\Omega_\mathrm{F}$.

Equation (3) also holds on each internal interface. The space of admissible stresses and displacements must account for singular stresses and displacement jumps, both represented by Dirac delta distributions whose support is $\partial\Omega_\mathrm{I}$. Indeed, to model the unilateral behaviour on the internal interfaces, it is required that the displacement field **u** can be singular on each $\partial\Omega_\mathrm{i}$, i.e. on $\partial\Omega_\mathrm{i}$ u can have a jump $\Delta\mathbf{u}^i$ that can be decomposed in its normal $\Delta\mathbf{u}_\mathrm{N}^i$ and tangential $\Delta\mathbf{u}_\mathrm{T}^i$ components [52]. Denoting with $|\Delta\mathbf{u}_\mathrm{T}^i|$ the L2 norm of the displacement jump in the tangential direction **t**, the friction condition with an associated behaviour reads:

$$\text{if } |\mathbf{S}_\mathrm{T}^i| \leq \mu|\mathbf{S}_\mathrm{N}^i| \text{ then } |\Delta\mathbf{u}_\mathrm{T}^i| = 0 , \tag{4}$$

$$\text{if } |\mathbf{S}_\mathrm{T}^i| = \mu|\mathbf{S}_\mathrm{N}^i|, \text{there exists } \lambda \geq 0 \text{ s.t. } \Delta\mathbf{u}_\mathrm{T}^i = -\lambda\mathbf{S}_\mathrm{T}^i \text{ and } \Delta\mathbf{u}_\mathrm{N}^i = -\lambda\mu\mathbf{S}_\mathrm{T}^i , \tag{5}$$

where μ is the friction coefficient, and $\mathbf{S}_\mathrm{N}^i$ and $\mathbf{S}_\mathrm{T}^i$ are the unknown, normal and tangential force distribution on $\Gamma_\mathrm{I}$. The stress tensor is symmetric and fulfils the following requirement:

$$\mathbf{T} \in \mathrm{C} , \tag{6}$$

where C is the convex Mohr-Coulomb cone. The set of admissible stress fields is:

$$\mathcal{H} = \{\mathbf{T} \in \mathrm{SBM} \,/\, \mathrm{div}\mathbf{T} + \mathbf{b} = \mathbf{0}, \mathbf{T} \in \mathrm{C}, \mathbf{s}(\mathbf{T}) = \bar{\mathbf{s}} \text{ on } \partial\Omega_\mathrm{F}\} . \tag{7}$$

A solution of the boundary value problem (BVP) is thus represented by a stress $\mathbf{T} \in \mathcal{H}$ and a displacement $\mathbf{u} \in \mathcal{K}$ fulfilling equations (25-26) also. It can be shown that for the problem at hand [54], using the Gauss-Green theorem, the following variational criterion can be derived:

$$\mathrm{A}(\mathbf{T}^*, \mathbf{T} - \mathbf{T}^*) \geq \int_{\partial\Omega_\mathrm{U}} \bar{\mathbf{u}} \cdot (\mathbf{Tn} - \mathbf{T}^*\mathbf{n})\mathrm{da}, \quad \forall\, \mathbf{T} \in \mathcal{H}_1 , \tag{8}$$

where **A** doubles the complementary elastic energy, and $\mathbf{T}^*$ corresponds to the boundary value problem solution. Relation (10) is equivalent to the following minimisation problem:

$$\mathbf{T}^* = \arg\min\{\Pi_\mathrm{c}(\mathbf{T})_{\mathbf{T}\in\mathcal{H}_1}\} , \tag{9}$$

with

$$\Pi_c(\mathbf{T}) = \frac{1}{2}\mathrm{A}(\mathbf{T},\mathbf{T}) - \int_{\partial\Omega_U} \bar{\mathbf{u}} \cdot \mathbf{Tn}\, \mathrm{da}\ , \tag{10}$$

where $\Pi_c(\mathbf{T})$ the total complementary energy (TCE). In the case of an associated flow-rule, the dual problem is represented by the total potential energy. Notably, if the cone $\mathrm{C}$ of (7) is assumed to be coincident with $Sym^+$, the previous formulation yields a typical Heyman problem.

## 3 NUMERICAL DISCRETISATION OF MINIMUM PROBLEM (9)

TCE minimum problem (9) is numerically discretised into the following Second-Order Cone Program adopting a typical concave formulation:

$$\begin{aligned} &\text{Minimise} \quad && -\mathbf{B}_s\, \mathbf{F}^T\, \bar{\mathbf{U}} + \mathbf{F}^T \mathbf{D}\, \mathbf{F} \\ &\text{s.t.} && \mathbf{A}_{eq}\, \mathbf{F} + \mathbf{b} = \mathbf{0} \\ & && \left\|\mathbf{f}_t^i\right\|_2 \leq \mu\, \mathbf{f}_n^i \quad for\ i = 1, \dots, n \end{aligned} \tag{11}$$

with:

- $n$ the total number of interfaces' nodes;
- $\mathbf{F}$ the vector collecting the internal nodal normal $\mathbf{f}_n^i$ and tangential $\mathbf{f}_t^i$ forces on the node $i$;
- $\bar{\mathbf{U}}$ the vector collecting the boundary displacement of the supports;
- $\mathbf{F}_s = \mathbf{B}_s\mathbf{F}$ the emerging stress vector obtained using the extract operator $\mathbf{B}_s$;
- $\mathbf{D}$ the compliance (deformability) matrix that takes the elastic block's compressive response into account;
- $\mathbf{A}_{eq}$ the equilibrium matrix; and,
- $\mathbf{b}$ the vector modelling the volume forces as lumped to the blocks' centroid.

Equation $(11)^2$ ensures that the elements are in equilibrium using the equilibrium matrix $\mathbf{A}_{eq}$, while equation $(11)^3$ represents the Mohr-Coulomb relationship between tangential and normal forces, scaled down by the friction coefficient $\mu$. There are $n$ second-order cone constraints represented by equation $(11)^3$, as the total number of nodes $n$. The objective function $(11)^1$ represents the TCE. The linear part represents the work on the boundary, i.e., is the opposite of the work done by the stresses and support displacements. The quadratic function enforces the elastic behavior of the interface using the compliance matrix $\mathbf{D}$, which considers different mechanical properties of the interface and their geometric distribution in the digital model.

If one neglects Equation (11) the problem yields a typical Heyman problem, as this is equivalent to assume a infinite friction capacity. Moreover, the quadratic part can be excluded, meaning that the contacts are assumed to be rigid. In this case, it provides exactly the dual formulation of the PRD problem for normal, rigid, no-tension, materials.

## 4 SEMICIRCULAR ARCH: NUMERICAL APPLICATIONS

This Section illustrates the method's potential on a semicircular arch considering different mechanical scenarios. The aim is to show how the minimum of the complementary energy provides an efficient numerical approach to computationally solve typical mechanical problem involving unilateral materials subjected to non-homogeneous boundary conditions. The geometry and its discretisation are depicted in **Fig. 2**. The semicircular arch has an internal radius of 1.00 m, a thickness of 0.20 m, a depth of 0.25 m and is discretised into 14 voussoirs. Two additional blocks are added as supports, and the boundary displacements are applied to their centroids. The computational time required to solve each SOCP problem is about 0.002 s.

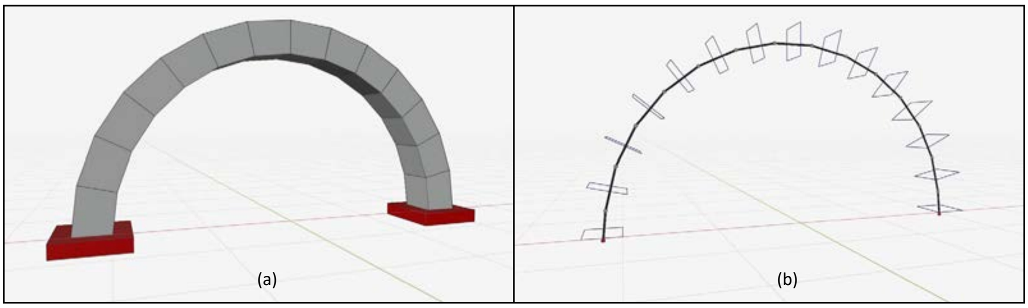


**Fig. 2** – The semicircular arch is discretised into 14 blocks, and two further blocks (in red) are added as supports: (a). In (b), the graph data structure.

### 4.1 Foundation settlements

This Section shows the TCE results when the semicircular arch is subjected to different foundation settlements. First, the mechanical response due to typical in-plane movements is explored. After that, a few meaningful out-of-plane foundation displacements are. The first analysis looks at the solution of a well-known mechanical problem: the minimum horizontal thrust problem (**Fig. 3**).

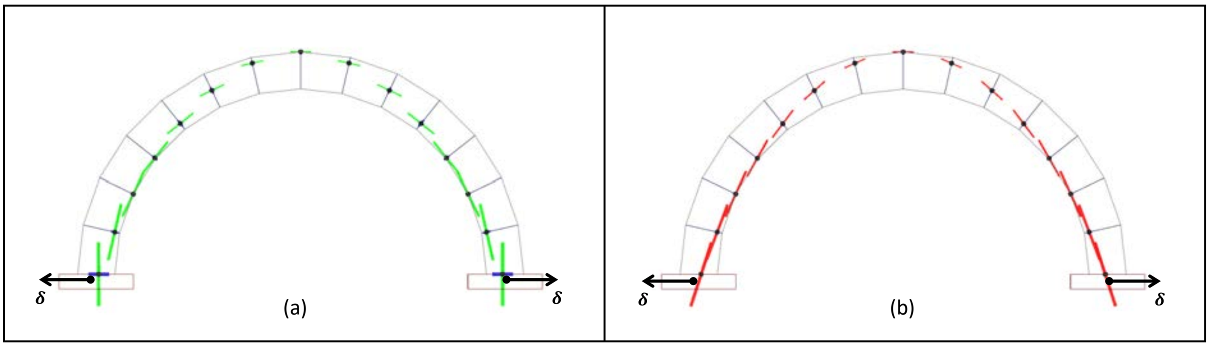


**Fig. 3** – Internal stress state for a small outward displacement: in (a) the results in terms of interface forces and torques (zero, in the present case); in (b) the interface resultant in red.

The two supports are subjected to a small, outward, horizontal displacement: the TCE solution provides nodal forces, which can be reduced to their interface resultants. The visualisation of the internal stress state through resultants offers a clear understating of the stress state: **Fig. 3b** shows a typical thrust line associated with the minimum thrust condition. The interface resultant in the middle span is touching the extrados, as expected. Also, note that the scalar product among the emerging singular stress field (thrust on the supports) and the small outward displacement is minimised (in the present case is positive). In **Fig. 4a-b**, two further, typical internal stress states are depicted. In **Fig. 4a**, the solution due to a small inward displacement results in the maximum thrust condition: the minimum work done by the inward displacements and the thrusts exerted on the supports is negative. **Fig. 4c-d** illustrate the internal stress states due to a small positive and negative rotation of the right support, respectively. The rotation is supposed to happen around the axis orthogonal to the plane of symmetry of the arch

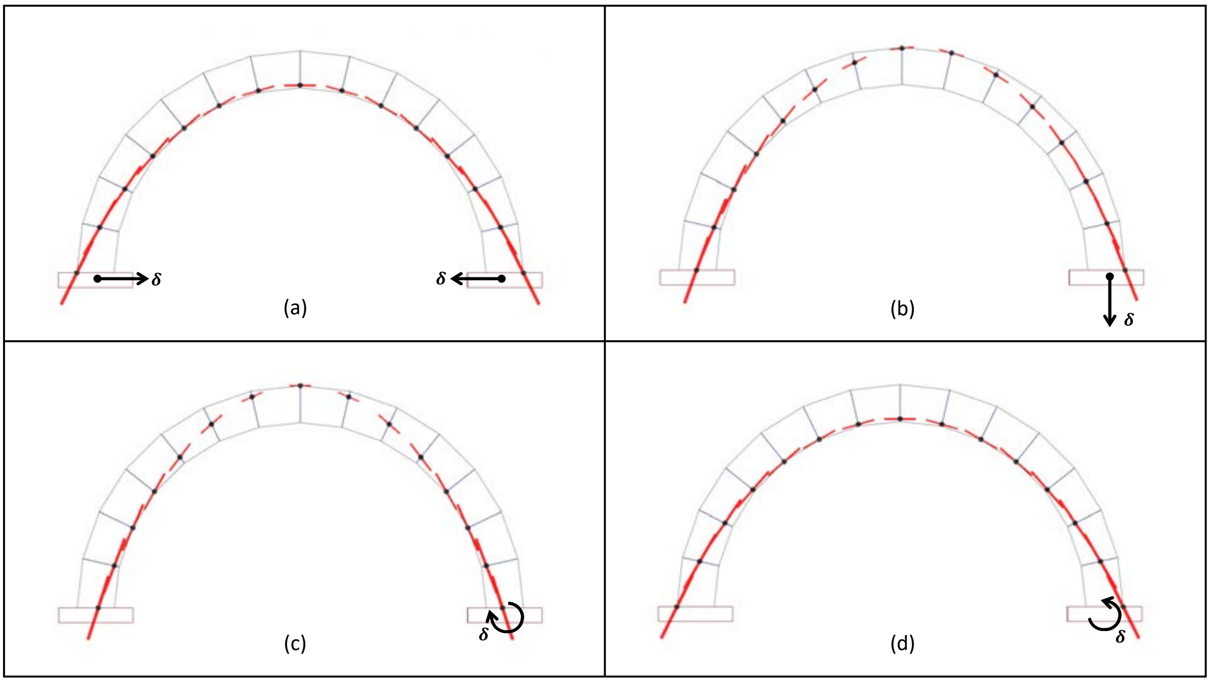


**Fig. 4** – Interface resultants minimising the TCE in four, different cases: in (a), a relative inward horizontal displacement is applied to both supports; in (b, c, d), the right support is subjected to a downward vertical displacement, to a negative and a positive rotation, respectively.

. Notably, as expected, the TCE criterion provides internal stress states corresponding to a minimum and maximum thrust condition. Thus, the minimum and maximum thrusts are not only connected to an inward or outward horizontal displacement, but other possible movements may activate these conditions.

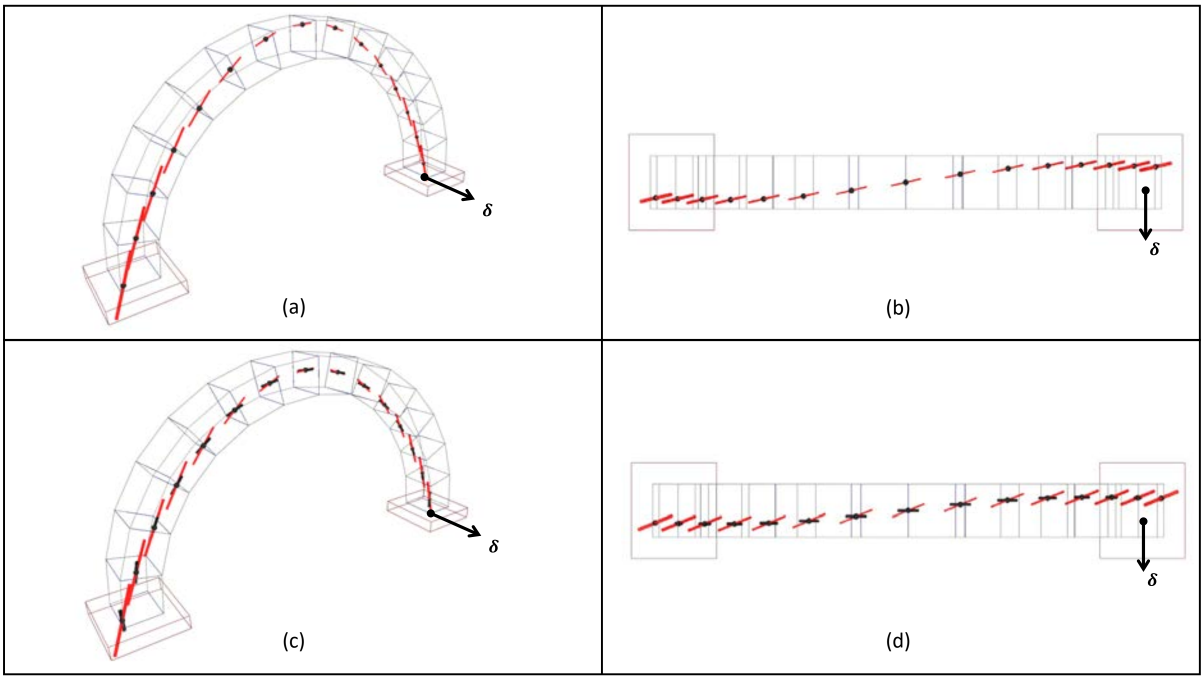


**Fig. 5** – The semicircular arch is subjected to relative transversal movement: internal stress states from (9) for $\mu = 0.8$ (first row) and $\mu = 2$ (second row). Beyond a slightly different pressure point positions, the second case provides torque resultants (in black) and higher tangential forces.

In all cases, the interface forces, as a measure of the internal stress state, return well-known thrust lines (the use of the term thrust line is not technically appropriate). These stress states are in a perfect agreement with the ones that can usually be found with classical, Heymanian Limit Analysis approaches. Nonetheless, it is pertinent to inquire about the internal, admissible stress state connected to relative transversal movements.

However, problem (9), when formulated in the space $Sym^{+}$, is unbounded. As soon as a finite friction capacity through additional friction constraints is introduced, the LP problem gets bounded, and an admissible stress state can be found. **Fig. 5** shows two different, admissible stress states evaluated using 0.8 and 2.0 as a friction coefficient μ. Specifically, the solution obtained for $\mu = 2$ offers transversal, friction forces higher than those corresponding to 0.8. Moreover, the solution shows also non-negligible torques. Also, the interface pressure points are slightly different.

**Fig. 6** depicts the internal stress state due to a transverse rotation of the right support is depicted. Even in the present case, problem (9) without friction constraints is not bounded meaning that this movement is not admissible for an Heymanian material, at least for the proposed discretisation.

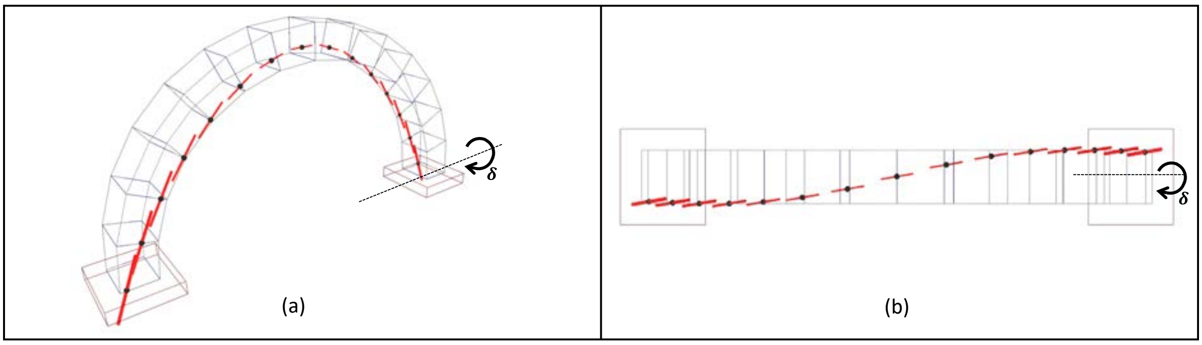


**Fig. 6** –The semicircular arch subjected to relative transversal, rotational movement: internal stress states for $\mu = 0.8$.

### 4.2 Seismic actions: lateral loads

The previous Section has shown typical cases of the arch subjected to its self-weight and to non-homogeneous foundation displacements. In the present Section, a classical load-bearing capacity analysis is provided increasing horizontal actions while still considering foundation displacements. The aim is to show how the TCE minimum can provide different solutions for increasing (but still safe) loading conditions and different foundation displacements. Solving the classical Limit Analysis problem (25) it is possible to evaluate the maximum horizontal multiplier λ for which the structure is still safe (just a little increment drives the system to a mechanism).

Looking at the in-plane response, the internal stress states solving for increasing horizontal multiplier's value are depicted in **Fig. 7**, considering two specific cases. On the right column, the arch is loaded by increasing horizontal forces. On the left column, an additional outward horizontal displacement is prescribed to the right support. As one can see, the internal stress state (see the pressure points) is influenced by the foundation displacement for $\lambda_0 < \lambda_0^{max}$. When $\lambda_0 = \lambda_0^{max}$, the two solutions coincide, because the limit state is unique.

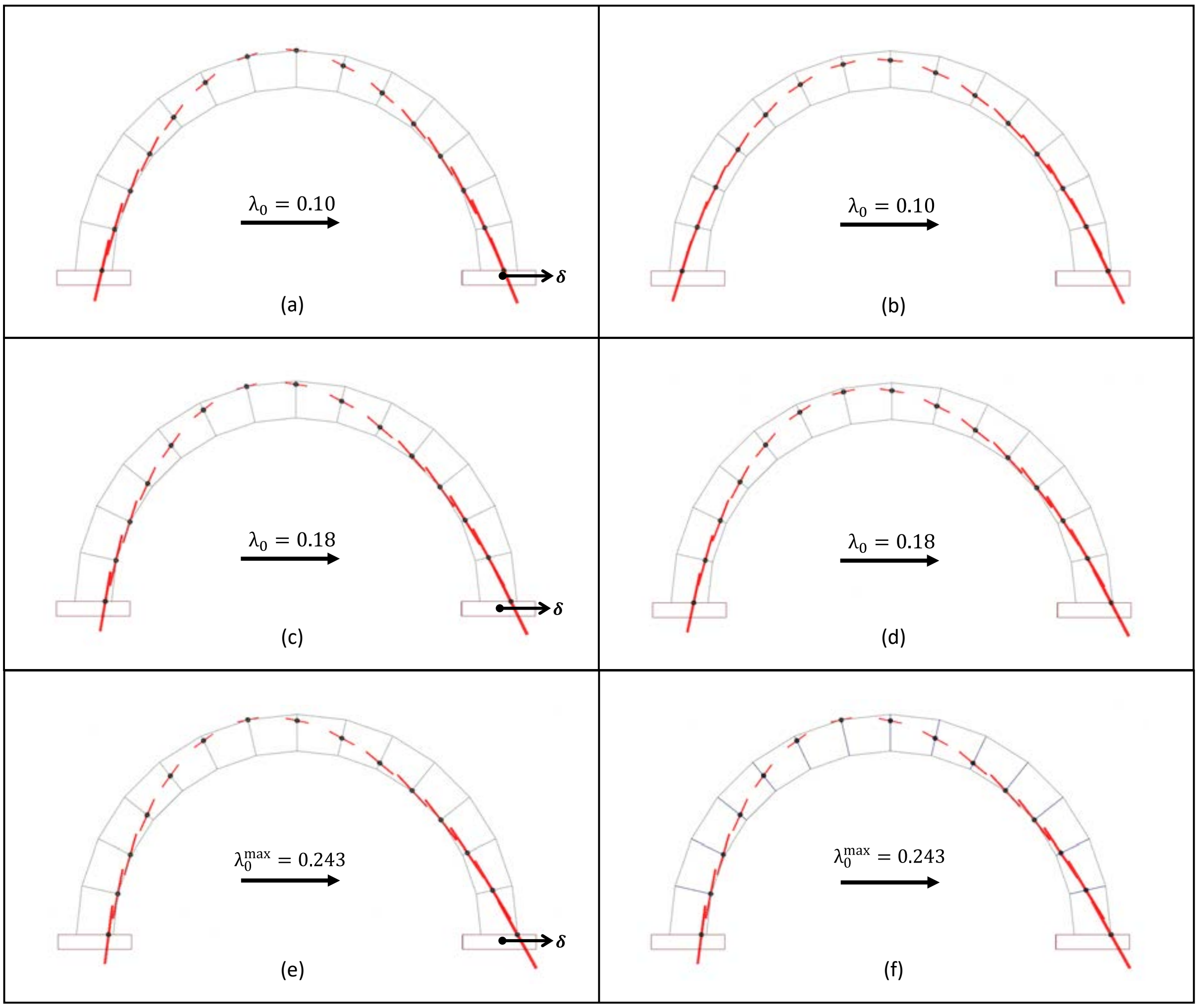


**Fig. 7** – The semicircular arch subjected to increasing loads (right) and to also an outward horizontal displacement (left): the foundation displacement strongly influences the internal stresses when $\lambda_0 < \lambda_0^{max}$.

To clearly illustrate this behaviour, **Fig. 8** reports the trend of the horizontal and vertical components of the thrust exerted on the supports for increasing in-plane horizontal loads and in three different cases: inward, outward and downward settling of the right support. When the horizontal, static multiplier reaches its maximum value ($\lambda_0^{max} = 0.243$), the arch is in a limit state condition, and the thrusts are the same.

Internal stress states solving the TCE problem for out-of-plane loading conditions and also considering different foundation settlements are reported in Fig. 9 with a focus on the limit state activated for $\lambda_{90}^{max} = 0.178$. The first row (Fig. 9a,b) depicts the internal stress state without considering foundation settlements. Conversely, the second (Fig. 9c,d) and third (Fig. 9e,f ) rows show the internal, limit stress states, taking into account two specific foundation displacements. In this particular case, the reader can see that the internal Limit stress state is not unique even though the horizontal (in the load direction) thrusts exerted to the supports have to be the same because of the equilibrium. The internal thrusts of Fig. 9 suggest that the collapse mechanism involves a global out-of-plane rocking around the base. This explains why the internal stress states are different: the rocking happens around the base interfaces' edges, and different pressure points lying on those edges are still compatible with the solution.

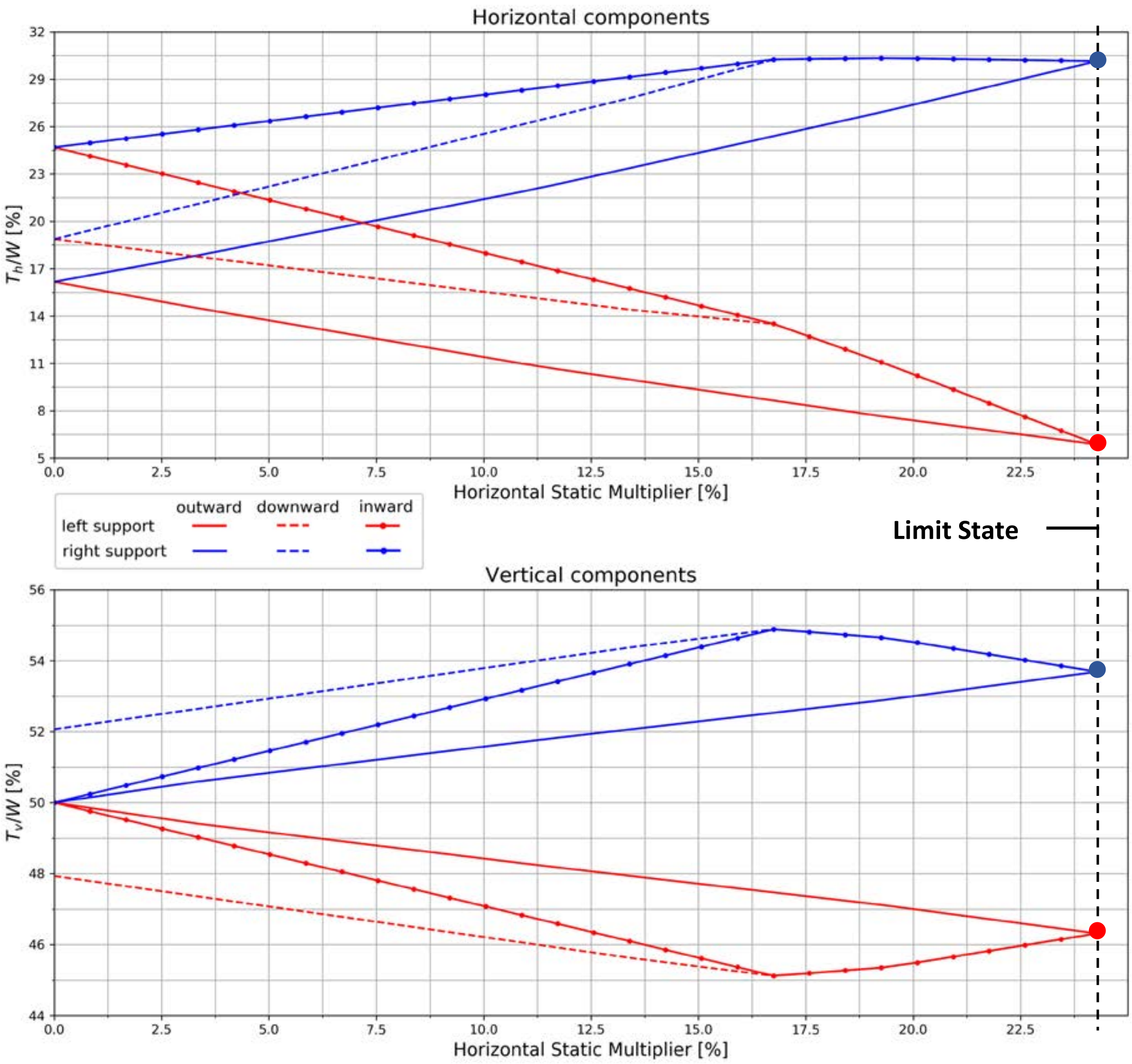


**Fig. 8** – Diagrams of horizontal and vertical components of the thrust exerted on the supports for increasing in-plane horizontal loads and in three different cases: inward, outward and downward settling of the right support. For $\lambda_0^{max} = 0.243$ the solutions are the same: the arch is in a limit state condition.

From a numerical point of view, it is evident that the limit state is dictated by the constraints of problem (11) (equilibrium and compatibility constraints). However, different energy solutions are still possible, meaning that the constraints do not define a single limit-state point, but the collapse's feasibility limit domain is infinite. In this sense, the objective function allows exploring this region also in a limit state condition.

## 5 CONCLUSIONS

The present paper proposes a novel 3D energy-based strategy to explore internal stress states in masonry structures modelled with a no-tension material. Different external actions and foundation displacements are considered. The problem is solved by the minimum of the total complementary energy (TCE), which is the variational criterion that selects equilibrated solutions compatible with boundary displacements. The TCE minimum was already adopted and benchmarked for 2D problems in [50, 51]. Here, this methodology is presented to 3D structures also considering material compatibility relations as coming from a Mohr-Coulomb failure criterion.

The structure is partitioned as an assembly of rigid elements, and the interaction among them

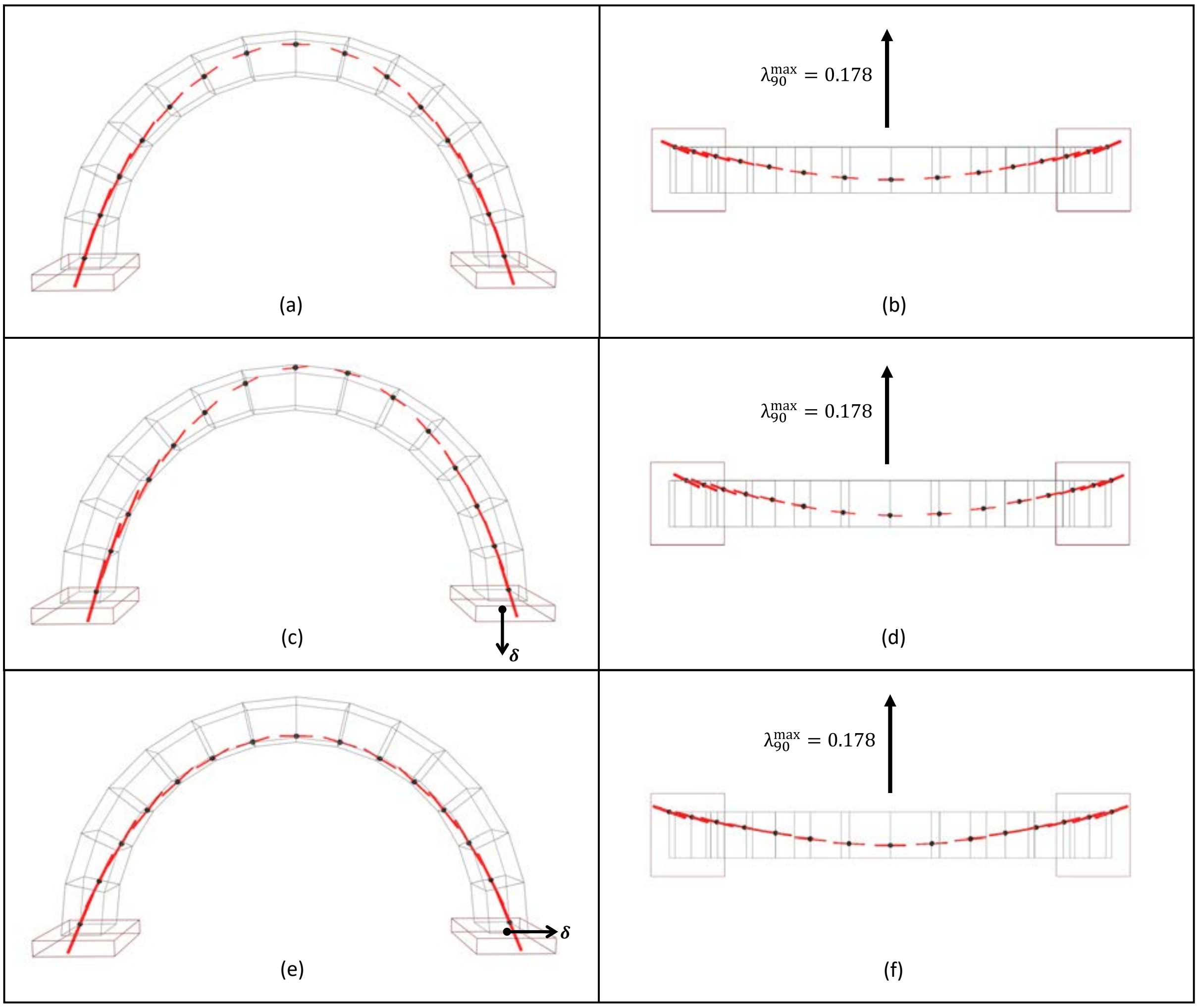


**Fig. 9** – The semicircular arch subjected to out-of-plane horizontal loads corresponding to $\lambda_{90}^{\max} = 0.178$. The second and third rows show the internal, Limit stress state due to two different foundation displacements. Note that the base pressure points are slightly different but still lying on the same interface edges.

is supposed to happen only on the interfaces' vertices as in a typical concave approach. The problem is discretized and can be solved in 2D as a LP or in 3D as a SOCP, as the Mohr-Coulomb cone is linear for plane problems or a cone for a fully 3D model. The objective function comprises a quadratic and a linear part. The last one represents the work among the emerging stresses at the boundary and the corresponding boundary displacements.

The method's potentials are illustrated on a semicircular arch paying particular attention to the influence of the material constraints. First, referring to a given structural partition, it is shown that typical Heymanian problems cannot be solved if the friction capacity is neglected as the corresponding LP or SOCP is unbounded. Once the material compatibly is introduced, the TCE problem becomes bounded. On a theoretical perspective, this observation provides a clear criterion to understand if displacement data are compatible with an Heymanian material model. Nonetheless, it is pertinent to inquire if the discretisation affects the solution, making the problem unbounded. By changing the discretisation or using a suitable (maybe continuous?) approach [55, 56, 57], can the corresponding TCE problem be bounded even using an Heymanian approach?

Second, it is illustrated how the boundary conditions drastically affect the internal stress states and redirect the flow of forces within the structure. Moreover, it is shown that the TCE minimum provides another strategy to solve a load-bearing capacity problem in an incremental way but still considering foundation settlements. Indeed, the incremental forces are increased in each step till the structure becomes unstable, while foundation settlements are used to active different internal stress states. The main outcome is that different internal force patterns/distributions in equilibrium with given external loads and compatible with different foundation settlements are possible. It is worth pointing out that the numerical method, as proposed, can be easily adapted to more complex 3D structures as the dome depicted in **Fig. 10**.

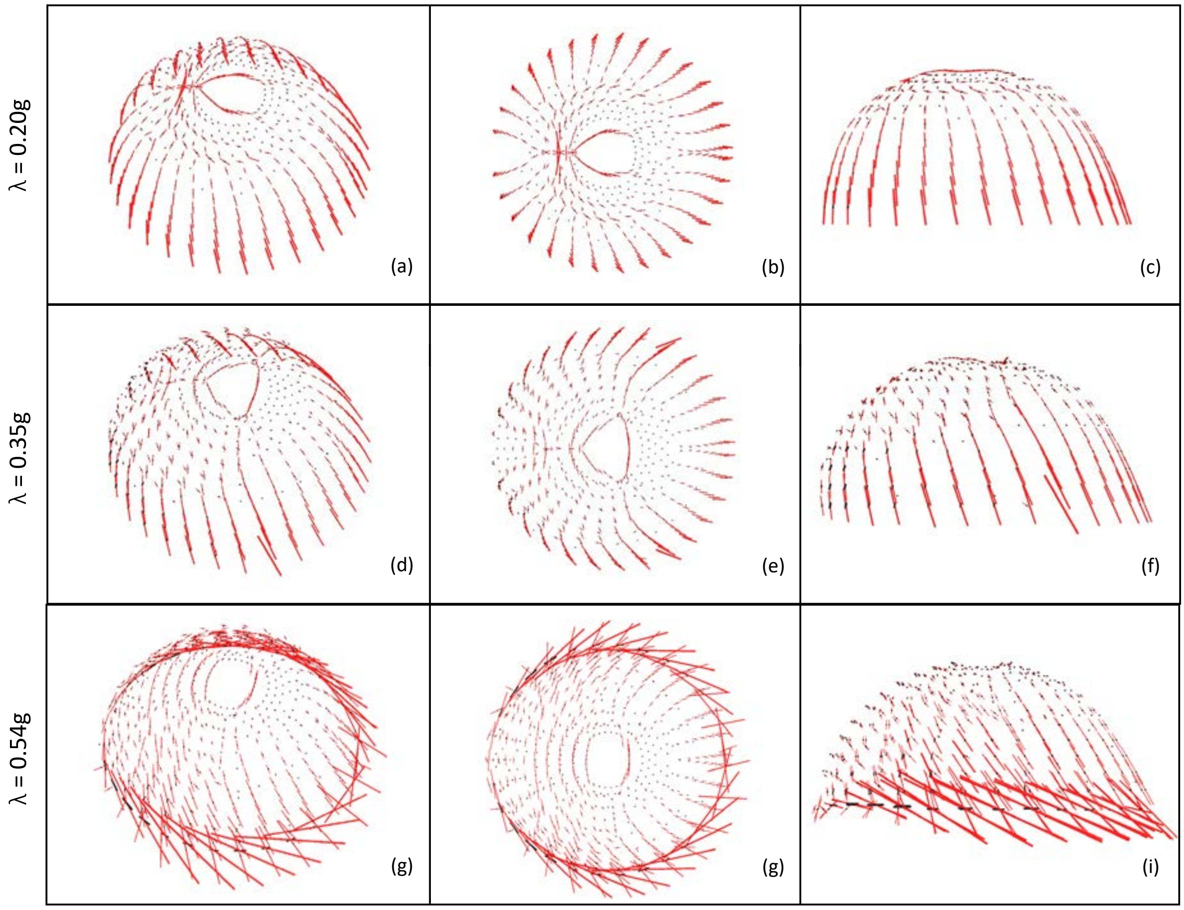


**Fig. 10** – A hemispherical dome subjected to a uniform, radial outward settlement and increasing horizontal loads: internal stress state corresponding to three different horizontal multipliers.

## ACKNOWLEDGMENTS

The research was funded by the Italian Ministry of University and Research through the Programme “Rita Levi Montalcini for young researchers” (FFO 2020).

## REFERENCES


[1] H.V. Shin, C.F. Porst, E. Vouga, J.A. Ochsendorf, F. Durand, Reconciling elastic and equilibrium methods for static analysis. *ACM Transactions on Graphics (TOG),* **35(2)**, 1-13, 2016.

[2] M. Monaco, M. Aurilio, A. Tufaro, M. Guadagnuolo, Sustainable Mortars for Application in the Cultural Heritage Field. *Materials,* **14(3)**, 598, 2021.

[3] P.B. Lourenço, J. G. Rots, Multisurface interface model for analysis of masonry structures. *Journal of engineering mechanics,* **123(7)**, 660-668, 1997.

[4] C. Baggio, P. Trovalusci, Discrete models for jointed block masonry walls. *The Sixth North American Masonry Conference,* **2**, 939-949, 1993.

[5] P. Zampieri, M. A. Zanini, F. Faleschini, L. Hofer, C. Pellegrino, Failure analysis of masonry arch bridges subject to local pier scour. *Engineering failure analysis,* **79**, 371-384, 2017.

[6] P.A. Cundall, A computer model for simulating progressive large scale movements in blocky rock systems. *Proceedings of the Symposium of the International Society of Rock Mechanics*, Nancy, France, 1971.

[7] J.V. Lemos, Discrete element modeling of masonry structures. *International Journal of Architectural Heritage,* **1(2)**, 190–213, 2007.

[8] V. Sarhosis, K. Bagi, J. Lemos, M. G, *Computational modeling of masonry structures using the discrete element method*, IGI Global, 2016.

[9] T. Forgács, V. Sarhosis, K. Bagi, Minimum thickness of semi-circular skewed masonry arches. *Engineering Structures,* **140**, 317-336, 2017.

[10] J. McInerney, M. J. DeJong, Discrete element modeling of groin vault displacement capacity. *International Journal of Architectural Heritage,* **9(8)**, 1037-1049, 2015.

[11] P. Meriggi, G. de Felice, S. De Santis, F. Gobbin, A. Mordanova, B. Pantò, Distinct Element Modelling of Masonry Walls under Out-Of-Plane Seismic Loading. *International Journal of Architectural Heritage,* **13(7)**, 1110-1123, 2019.

[12] F. Gobbin, G. de Felice, J. V. Lemos, A Discrete Element Model for Masonry Vaults Strengthened with Externally Bonded Reinforcement. *International Journal of Architectural Heritage,* **15(12)**, 1959-1972, 2020.

[13] F. Portioli, C. Casapulla, L. Cascini, An efficient solution procedure for crushing failure in 3D limit analysis of masonry block structures with non-associative frictional joints. *International Journal of Solids and Structures,* **69**, 252-266, 2015.

[14] M. Gilbert, C. Melbourne, Rigid-block analysis of masonry structures. *Structural engineer,* **72(21)**, 1994.

[15] M. Gilbert, C. Casapulla, H. M. Ahmed, Limit analysis of masonry block structures with non-associative frictional joints using linear programming. *Computers & structures,* **84(13-14)**, 873-887, 2006.

[16] F. Portioli, C. Casapulla, M. Gilbert, L. Cascini, Limit analysis of 3D masonry block structures with non-associative frictional joints using cone programming. *Computers and Structures,* **143**, 108-121, 2014.

[17] A. Orduña, P. B. Lourenço, Three-dimensional limit analysis of rigid blocks assemblages. Part I: Torsion failure on frictional interfaces and limit analysis formulation. *International Journal of Solids and Structures,* **42(18-19)**, 5140-5160, 2005.

[18] R. Livesley, Limit analysis of structures formed from rigid blocks. *International Journal for Numerical Methods in Engineering,* **12(12)**, 1853-1871, 1978.

[19] R.K. Livesley, A computational model for the limit analysis of three-dimensional masonry structures. *Meccanica,* **27(3)**, 161-172, 1992.

[20] J. Heyman, The stone skeleton. *International Journal of solids and structures,* **2(2)**, 249-279, 1966.

[21] S. Huerta Fernández, Geometry and equilibrium: The gothic theory of structural design. *Structural Engineer,* **84(2)**, 23-28, 2006.

[22] S. Huerta Fernández, Galileo was wrong: the geometrical design of masonry arches. *Nexus Network Journal,* **8(2)**, 25-52, 2006.

[23] S. Coccia, M. Como, F. Di Carlo, Wind strength of gothic cathedrals. *Engineering failure analysis,* **55**, 1-25, 2015.

[24] P. Block, J. A. Ochsendorf, Thrust network analysis: A new methodology for three-dimensional equilibrium, *Journal of the International Association for shell and spatial structure,* **48(3)**, 167-173, 2007.

[25] P. Block, L. Lachauer, Three-dimensional (3D) equilibrium analysis of gothic masonry vaults. *International Journal of Architectural Heritage,* **8(3**), 312-335, 2014.

[26] P. Block, L. Lachauer, Three-dimensional funicular analysis of masonry vaults. *Mechanics Research Communications,* **56**, 53-60, 2014.

[27] F. Marmo, D. Masi, L. Rosati, Thrust network analysis of masonry helical staircases. *International Journal of Architectural Heritage,* 1-21, 2018.

[28] C. Olivieri, S. Adriaenssens, C. Cennamo, A novel graphical assessment approach for compressed curved structures under vertical loading. *International Journal of Space Structures,* **09560599231161424**, 2023.

[29] M. Angelillo, A. Bortot, C. Olivieri, The Corner Tower of Anagni Cathedral: Geometry and Equilibrium. *Nexus Network Journal,* 1-9, 2023.

[30] F. Fraternali, M. Angelillo, A. Fortunato, A lumped stress method for plane elastic problems and the discrete-continuum approximation. *International journal of solids and structures,* **39(25)**, 6211–6240, 2002.

[31] F. Fraternali, A thrust network approach to the equilibrium problem of unreinforced masonry vaults via polyhedral stress functions. *Mechanics Research Communications,* **37(2)**, 198-204, 2010.

[32] E. De Chiara, C. Cennamo, A. Gesualdo, A. Montanino, C. Olivieri, A. Fortunato, Automatic generation of statically admissible stress fields in masonry vaults. *Journal of Mechanics of Materials and Structures,* **14(5)**, 719-737, 2019.

[33] A. Gesualdo, G. Brandonisio, A. De Luca, A. Iannuzzo, A. Montanino, C. Olivieri, Limit analysis of cloister vaults: the case study of Palazzo Caracciolo di Avellino. *Journal of Mechanics of Materials and Structures,* **14(5)**, 739-750, 2019.

[34] A. Montanino, C. Olivieri, G. Zuccaro, M. Angelillo, From stress to shape: Equilibrium of cloister and cross vaults. *Applied Sciences,* 11(9), 3846, 2021.

[35] C. Cusano, A. Montanino, C. Olivieri, V. Paris, C. Cennamo, Graphical and analytical quantitative comparison in the Domes assessment: The case of San Francesco di Paola. *Applied Sciences,* **11(8)**, 3622, 2021.

[36] C. Cusano, A. Montanino, C. Cennamo, G. Zuccaro and M. Angelillo, Geometry and stability of a double-shell dome in four building phases: the case study of Santa Maria Alla Sanità in Naples. *International Journal of Architectural Heritage,* **17(2)**, 2023.

[37] M. Monaco, I. Bergamasco, M. Betti, A no-tension analysis for a brick masonry vault with lunettes. *Journal of Mechanics of Materials and Structures,* **13(5)**, 703-714, 2018.

[38] M. Monaco, B. Calderoni, A. Iannuzzo, A. Gesualdo, Behaviour of in-plane loaded masonry panels. *Procedia Structural Integrity,* **11**, 388-393, 2018.

[39] A. Geusaldo, B. Calderoni, A. Sandoli, M. Monaco, Minimum energy approach for the in-plane shear resistance of masonry panels. *Ingegneria Sismica,* **36(1)**, 42-53, 2019.

[40] A. Gesuado, B. Calderoni, A. Iannuzzo, A. Fortunato, M. Monaco, Minimum energy strategies for the in-plane behaviour of masonry. *Frattura ed Integrità Strutturale,* **14(51)**, 376-385, 2020.

[41] A. Fortunato, A. Gesualdo, I. Mascolo, M. Monaco, P-Bézier energy optimisation for elastic solutions of masonry-like panels. *International Journal of Masonry Research and Innovation,* **7(1-2)**, 113-125, 2022.

[42] S. Acikgoz, K. Soga, J. Woodhams, Evaluation of the response of a vaulted masonry structure to differential settlements using point cloud data and limit analyses. *Construction and Building Materials,* **150**, 916-931, 2017.

[43] A.M. D'Altri, S. De Miranda, G. Castellazzi, V. Sarhosis, J. Hudson, D. Theodossopoulos, Historic barrel vaults undergoing differential settlements. *International Journal of Architectural Heritage,* 1-14, 2019.

[44] M. Pepe, M. Sangirardi, E. Reccia, M. Pingaro, P. Trovalusci, G. de Felice, Discrete and Continuous Approaches for the Failure Analysis of Masonry Structures Subjected to Settlements. *Frontiers in Built Environment,* **6(43)**, 2020.

[45] A. Spada, The effect of vertical ground movement on masonry walls simulated through an elastic–plastic interphase meso-model: a case study. *Archive of Applied Mechanics,* **89(8)**, 1655-1676, 2019.

[46] M.J. DeJong, Settlement effects on masonry structures. *Proceedings of the 10th International Conference on Structural Analysis of Historical Constructions, SAHC 2016*, 449-456, 2016.

[47] S. Coccia, F. Di Carlo, Z. Rinaldi, Collapse displacements for a mechanism of spreading-induced supports in a masonry arch. *International Journal of Advanced Structural Engineering,* **7(3)**, 307-320, 2015.

[48] A. Montanino, D. De Gregorio, C. Olivieri, A. Iannuzzo, The continuous Airy-based for stress-singularities (CASS) method: an energy-based numerical formulation for unilateral materials. *International Journal of Solids and Structures,* **256**, 2022.

[49] M. Angelillo, A. Fortunato, A. Gesualdo, A. Iannuzzo, G. Zuccaro, Rigid block models for masonry structures. *International Journal of Masonry Research and Innovation,* **3(4)**, 349-368, 2018.

[50] A. Iannuzzo, T. Van Mele, P. Block, Piecewise Rigid Displacement (PRD) method: A limit analysis-based approach to detect mechanisms and internal forces through two dual energy criteria. *Mechanics Research Communications,* **107**, doi:103557, 2020.

[51] A. Iannuzzo, A. Dell'Endice, T. Van Mele, P. Block, Numerical Limit Analysis-based modelling of masonry structures subjected to large displacements. *Computers & Structures,* **242**, 106372, 2020.

[52] A. Iannuzzo, M. Angelillo, E. De Chiara, F. De Guglielmo, F. De Serio, F. Ribera, A. Gesualdo, Modelling the cracks produced by settlements in masonry structures. *Meccanica,* **53(7)**, 1857-1873, 2018.

[53] F. Perelli, D. De Gregorio, A. Montanino, C. Olivieri, G. Maddaloni, A. Iannuzzo, Energy-based modelling of in-plane fragility curves for the 2D ultimate capacity of Italian masonry buildings. *Frontiers in Built Environment,* **9**, 1127523, 2023.

[54] C. Olivieri, A. Iannuzzo, A. Fortunato, M.J. DeJong, The effect of concentrated loads on open-well masonry spiral stairs. *Engineering Structures,* **272**, 114952, 2022.

[55] A. Iannuzzo, Energy based fracture identification in masonry structures: the case study of the church of "Pietà dei Turchini". *Journal of Mechanics of Materials and Structures,* **14(5)**, 683-702, 2019.

[56] A. Iannuzzo, P. Block, M. Angelillo, A. Gesualdo, A continuous energy-based numerical approach to predict fracture mechanisms in masonry structures: CDF method. *Computers & Structures,* **257**, 106645, 2021.

[57] I. Mascolo, A. Gesualdo, C. Olivieri, A. Fortunato, On blocks detection in unilateral masonry-like structures: a rigid-elastic displacement approach. *International Journal of Masonry Research and Innovation,* **7(4)**, 395-405, 2022.